Enhanced removal of Cr(VI) by polymer inclusion membrane based on poly(vinylidene fluoride) and Aliquat 336

Ferhat Sellami, Ounissa Kebiche-Senhadji, Stéphane Marais, Laurent Colasse, Kateryna Fatyeyeva

Enhanced removal of Cr(VI) by polymer inclusion membrane based on poly(vinylidene fluoride) and Aliquat 336

Ferhat Sellami[1,2], Ounissa Kebiche-Senhadji[1], Stéphane Marais[2], Laurent Colasse[2], Kateryna Fatyeyeva[2*]

[1]*Laboratoire de procédés membranaires et de technique de séparation et de récupération (LPMSTR), Université de Bejaia, Targa Ouzemour 06000, Bejaia, Algeria*

[2]*Normandie Univ., UNIROUEN, INSA ROUEN, CNRS, Polymères, Biopolymères, Surfaces (PBS), 76000 Rouen, France*

*corresponding author: kateryna.fatyeyeva@univ-rouen.fr

Abstract

New polymer inclusion membranes (PIMs) based on poly(vinylidene fluoride) (PVDF) (polymer matrix), tricaprylmethylammonium chloride (Aliquat 336) (ion carrier) and 2-nitrophenyloctylether (2NPOE) (plasticizer) were successfully elaborated by casting evaporation method and used in selectively facilitated transport of Cr(VI) ions in an acidic aqueous medium. Obtained PIMs are dense and homogeneous and are characterized by intermolecular interactions of the membrane components (i.e. polymer matrix, ion carrier and plasticizer). The presence of ion carrier and plasticizer enhances the membrane flexibility and its hydrophilic character. The decrease of the PVDF melting point is ascribed to the strong electrostatic interactions between liquid compounds (i.e. ion carrier and plasticizer) and polymer chains. PVDF-based PIM with only 20 wt.% of Aliquat 336 ensures almost complete transport of Cr(VI) ions from the donor to acceptor phase. Moreover, the addition of 5 wt.% of plasticizer significantly increases the transport flux. Also, Cr(VI) ions are selectively recovered (~97%) from a mixture containing other heavy metal ions (Cd(II), Pb(II), Fe(III), Zn(II), Cu (II), Ni(II), Co(II)) with such PIM. Elaborated PVDF-based PIMs reveal improved transport properties compared to other polymer-based PIMs, exhibiting high stability (more than 190h) and lifetime durability and so they are suitable for long term application.

Keywords: polymer inclusion membrane (PIM), poly(vinylidene fluoride) (PVDF), Aliquat 336, Cr(VI) extraction, lifetime durability.

1. Introduction

Chromium (Cr) is a common heavy metal pollutant in water, where it mainly exists in two stable oxidation states, namely, hexavalent chromium (Cr(VI)) and trivalent chromium (Cr(III)). The hexavalent chromium is chosen as a target molecule because of its high hazard [1]. Toxicity studies have shown that Cr can enter the human body through the respiratory tract and skin, thus having significant carcinogenic and mutagenic effects. Cr(VI) is about 100 times more toxic than Cr(III) because of its higher solubility and easy absorption and accumulation in kidneys, stomach, and liver [2]. Cr-containing compounds have a wide range of industrial sources, such as tannery, cooling tower discharge, electroplating and electrolysis. More than 170 000 tons of chromium wastes are let to go into the environment worldwide each year [3]. Thus, Cr-containing wastewater is one of the major environment pollutants [4]. The emission limit of industrial chromium is less than 1 mg/L [5], whereas according to the United States Environmental Protection Agency, the maximum allowable limit for Cr(VI) in inland water and in drinking water is 0.1 and 0.05 mg/L, respectively [6].

Various methods have been developed for the Cr(VI) removal from wastewater, e.g. filtration membrane, ion exchange, reverse osmosis, precipitation, electrochemical treatment, solvent extraction, adsorption/biosorption, and others [7-10]. The extractants, which are able to interact with metals, can be used to facilitate metal removal. In this sense, ionic liquids (ILs) can be applied as heavy metal extracting agents [11]. ILs are a class of salts that are liquid at room temperature and under 100°C. They consist of an organic cation and an organic or inorganic anion, and possess unique properties that make them a good alternative in comparison with common organic solvents [11]. The ILs use as extracting agents for efficient removal of metal ions can be successful by proper selection of the anion, which is supposed to bind to the respective metal ions.

Polymer inclusion membranes (PIMs) have recently attracted attention for the separation of metal ions and small organic compounds from their aqueous solutions [7, 12]. PIMs are one of the types of liquid membranes where the extractant (often referred to as ion carrier) and a plasticizer (if present in the PIM composition) are immobilized between the entangled chains of the membrane base polymer [7]. It should be mentioned that the majority of the extractants used as carriers in PIMs have plasticizing properties and there is no need to add separate plasticizers to the membrane composition [12, 13]. PIMs have grown in popularity due to the ease of their preparation and use and their better stability compared to supported liquid membranes (SLMs), which are still the most popular type of liquid membranes. The separation process using PIM is an attractive green alternative to traditional solvent extraction methods as an organic solvent is not required and a much smaller amount

of the extractant is needed [7, 13-16]. Moreover, the PIM application allows extraction and stripping processes to run at the same time, hence increasing the extraction efficiency.

PIMs are generally prepared by casting a solution containing a base polymer, an extractant (ion carrier) and a plasticizer. After the solvent evaporation, a stable and flexible thin film is formed. Owing to the compatibility with the majority of extractants, cellulose triacetate (CTA) and poly(vinylchloride) (PVC) are the most used polymers for the PIM elaboration [7, 17]. However, CTA and PVC have some drawbacks that limit their stability and reuse in several cycles. Indeed, CTA is prone to be hydrolyzed in strongly acid and alkaline solutions that leads to a loss of the carrier and plasticizer [18, 19]. In its turn, PVC is liable to undergo the dehydrochlorination in alkaline conditions and becomes black [20]. But the most important drawback is the fact that in order to ensure an effective transport, a large amount of plasticizer should be used in the case of CTA- and PVC-based membranes [21, 22].

To solve the problem of stability in aqueous and alkaline medium of CTA- and PVC-based PIMs, new more stable membranes should be designed. Poly(vinylidene fluoride)(PVDF) is a semi-crystalline polymer with repeated unit of–$(CH_2CF_2)_n$–. It has a glass transition temperature T_g of around -39°C and exhibits high mechanical strength, good chemical resistance and thermal stability as well as excellent aging resistance, which is very important for the industrial application of separation membranes [23]. Up to now, PVDF membranes are used for water filtration, recovery of biofuels *via* pervaporation process, as a separator in lithium ion battery, as a support for composite membranes, and so on [23, 24].

During the last decade, new PIMs were elaborated using PVDF and its copolymers – poly(vinylidene fluoride-*co*-tetrafluoroethylene) (PVDF-*co*-TFE) and poly(vinylidene fluoride-*co*-hexafluoropropylene) (PVDF-*co*-HFP) [16, 25-31]. Guo et al. designed a microporous membrane based on PVDF and PVDF-*co*-TFE and ionic liquids for hexavalent chromium and rare earths removal using the phase inversion technique [25, 26]. O'Bryan et al. used PVDF-*co*-HFP and Aliquat 336 for the dense PIMs elaboration by means of the solvent evaporation technique [28]. PVDF-*co*-HFP was also combined with Cyphos IL 104 [16], Cyphos IL 101 [29] and imidazolium bromide-based room temperature ionic liquids [30] or with LIX 84I [31] to obtain dense PIMs with excellent stability during extraction and back extraction experiments.

The physical and chemical properties of PIMs based on PVDF and its copolymers strongly depend on the preparation techniques. For example, O'Bryan et al. revealed that the properties of PVDF-*co*-HFP/Aliquat 336 membranes obtained by the phase inversion technique and by solvent evaporation casting technique were different [28]. Moreover, the

solvent nature and its evaporation temperature as well as the polymer concentration may also affect the membrane properties and their structure [32-34]. Bonggotgetsakul et al. obtained the membrane based on PVDF and Cyphos IL104 by solution evaporation technique using tetrahydrofuran (THF) as a solvent [16]. They found that in that case an inhomogeneous membrane was obtained.

In contrast with well characterized CTA- and PVC-based PIMs, the research dealing with PVDF-based PIMs is mainly focused on the optimization of the membrane composition for the efficient extraction of the desired species. And to our knowledge, the physical and chemical properties of dense PVDF-based PIMs are not investigated concerning their structure and extraction ability. Therefore, PIMs based on PVDF, Aliquat 336 and 2NPOE are designed and characterized in the present work. The composition of elaborated membranes was optimized in terms of efficient removal of Cr(VI) from aqueous solutions and the extraction and removal performance was compared with the behaviour of common PIMs based on CTA and PVC. The influence of the ion carrier and plasticizer on the membrane properties was studied by thermal (differential scanning calorimetry (DSC) and thermogravimetric analysis (TGA)), surface (contact angle, scanning electron microscopy (SEM) and infrared spectroscopy) and mechanical analysis. The obtained results were correlated with the membrane transport behaviour. In addition, the durability study was carried out in order to detect the leakage of the liquid phase (i.e. ion carrier and plasticizer) from the membrane and/or any changes of the membrane structure during the storage for 18 months.

2. Experimental part

2.1. Chemicals

CTA pellets with 43-49 wt.% acetyl, PVC powder (M_w = 43 000 g/mol), Aliquat 336(≥ 97% purity), 2NPOE (≥99% purity), chloroform (99.0-99.4% purity) and hydrochloric acid were received from Sigma-Aldrich. PVDF powder was purchased from Alfa Aesar.1.5-diphenylcarbazide (DPC) (≥97% HPLC purity) obtained from Fluka chemika, N,N-dimethylformamide (DMF) (≥ 99.8% purity), acetic acid (≥ 99.5% purity) and ammonium acetate (≥ 98% purity) provided by Biochem, THF (99.9% purity) received from VWR chemicals, potassium chromate K_2CrO_4 (99.5% purity) obtained from Acros and sodium hydroxide NaOH (99% purity) purchased from Merck were used without further purification.

All water used in the work was milli-Q water (Milli-Q Water System, Millipore, resistivity = 18 MΩ·cm at 25°C).

2.2. Membrane preparation

PVDF-based PIMs were prepared by casting and solvent evaporation technique. For this purpose, PVDF was dissolved in DMF (1 g of polymer in 10 mL of DMF) under magnetic stirring at room temperature (25 ± 2°C) to complete polymer solubility. Then, the required amounts of carrier and plasticizer were added and the mixture was further stirred to obtain a homogenous solution. The obtained solution was poured onto the flat glass plate using an automatic film applicator (Sheen 1137 with a casting knife of 200 µm). Finally, the plate with a casted solution was placed in an oven at 60°C and DMF was allowed to evaporate slowly for at least 72h. Resulting PIMs were then peeled off from the glass plate for further analysis and characterization. In the case of CTA- and PVC-based PIMs, DMF was replaced by chloroform and THF, respectively. The casting solutions (1 wt.% polymer) containing a plasticizer and ion carrier were poured onto Petri dish and covered to allow slow solvent evaporation at room temperature (25 ± 2°C) during 72h.

For clarity, XPVDF/YAliquat 336/Z-2NPOE refers to the membrane with a certain amount of PVDF, Aliquat 336 and 2NPOE. The values of X, Y and Z represent the PVDF, Aliquat 336 and 2NPOE amount, respectively, expressed in wt.%.

2.3. Physical and chemical characterization

2.3.1 Spectroscopy measurements

The FTIR spectra were recorded on Thermo Nicolet Is50 FTIR spectrophotometer equipped with a diamond crystal in attenuated total reflectance (ATR) mode. A series of 256 scans was collected for each membrane over the 4000–400 cm^{-1} spectral range with a 4cm^{-1} resolution.

The Cr(VI) concentration in transport experiments was analyzed in acidic medium using an UV–Visible spectrophotometer at 540 nm (ThermoFisher Evolution 220).

The mixture metal ions concentration was determined using inductively coupled plasma spectrometer (ICPThermo ICP 7000 Series).

2.3.2. Tensile tests

Mechanical measurements were performed on Instron 5543 equipped with the 500 N load cell. Tensile tests were carried out using normalized specimens (type 5A) according to

ISO 527-2. The specimens were stretched to the main axis at 1 mm/min at room temperature (25 ± 1°C) and hygrometry (34 ± 4% relative humidity). At least five samples were tested for each membrane composition.

2.3.3. Contact angle

The water contact angle θ was measured using a sessile drop method by Multiskop goniometer (Optrel, Germany). For this, water was dropped on the membrane using a micro syringe and photographed with a black and white CCD camera (0.8 magnification lens). At least five drops were analyzed at different membrane locations at room temperature (25 ± 1°C) and hygrometry (34 ± 2% relative humidity).

2.3.4. Differential scanning calorimetry

DSC measurements were performed by means of the Polyma apparatus from Netzsch. All the experiments were performed in an aluminum pan with pierced lid in the nitrogen atmosphere from -50°C to 200°C at the heating rate of 10°C/min. The results were analyzed with Proteus software.

2.3.5. Thermogravimetric analysis

The membrane thermal behavior was studied using the TGA analyzer (TGA Q500, TA Instruments, USA). The TGA measurements were carried out from 30°C to 800°C in the nitrogen atmosphere. The heating rate and the nitrogen flow rate were 10°C/min and 90 mL/min, respectively.

2.3.6. Scanning electron microscopy

For structural characterization, the membrane morphology was observed with a Zeiss EVO 40 scanning electron microscope. Samples were fractured in liquid nitrogen and covered with a carbon layer before observations.

2.4. Transport performance

All experiments were carried out using a Teflon permeation cell composed of two equal (200 mL) cylindrical compartments (diameter: 6cm, height: 8.5 cm) at room temperature (25 ± 1°C). The membrane (diameter: 4 cm) was sandwiched between these two compartments. A Cr(VI) solution in 0.1M HCl was used as the donor phase and the acceptor phase solution was buffered by a solution of acetic acid and ammonium acetate at pH 5 or by

a solution of 0.1 M NaOH. Each solution was mechanically stirred at 1000 rpm. The samples were taken periodically from the both compartments with a micropipette and analyzed.

The kinetic transport parameters were calculated according to:

$$\ln(\frac{C_{donor}}{C_{0donor}}) = -kt, \quad (1)$$

where C_{donor} is the Cr(VI) concentration in the donor phase at time *t* and C_{0donor} is the initial Cr(VI) concentration in the donor phase (i.e. at $t = 0$).

The relationship $\ln(\frac{C_{donor}}{C_{0donor}})$ versus time was linear, that was confirmed by the values of the determination coefficient (R^2) close to 1 (i.e. 0.99).The permeability coefficient *P* was calculated as follows:

$$P = \frac{V}{A}\,k, \quad (2)$$

Where *V* is the volume of the aqueous donor solution, and *A* is the active membrane area. The initial flux J_i is determined using:

$$J_i = PC_i \quad (3)$$

The percentage of metal ions transported from the donor to acceptor phase (i.e. recovery factor) is defined as:

$$R(\%)_{acceptor\ phase} = \frac{C_{t\ acceptor}}{C_{Odonor}} \cdot 100, \quad (4)$$

where $C_{t\ acceptor}$ is the Cr(VI) concentration in the acceptor phase at time *t.*

The percentage of metal ions accumulated in the membrane phase (i.e. accumulation factor) is defined as:

$$A\ (\%)_{membrane\ phase} = \frac{C_{t\ membrane}}{C_{Odonor}} \cdot 100, \quad (5)$$

where $C_{t\ membrane}$ is the Cr(VI) concentration in the membrane phase at time *t* equal to $C_{t\ membrane} = C_{0\ donor} - (C_{t\ donor} + C_{t\ acceptor})$.

The percentage of metal ions removed from the donor phase (so-called removal factor) is determined according to:

$$R(\%)_{donor\ phase} = \frac{C_{Odonor} - C_{t\ donor}}{C_{Odonor}} \cdot 100 \quad (6)$$

3. Results and discussion

Prior to further analysis, the elaborated PVDF-based membranes were visually examined. It is stated that they are homogeneous, smooth, flat and rather transparent whatever the membrane composition (i.e. Aliquat 336 and 2NPOE content). The addition of high

concentration of the ionic liquid (Aliquat 336) and the plasticizer (2NPOE) leads to membranes with a slightly translucent appearance.

3.1. Physical and chemical characterization of PVDF-based membranes

3.1.1. Spectral behaviour

In order to reveal possible interactions of membrane different components (i.e. polymer, ionic liquid and plasticizer), FTIR analysis was carried out and the obtained spectra are shown in **Fig. 1**. The spectra for pure membrane components are given for comparison. The spectrum of Aliquat 336 is characterized by two bands at 2922 $cm^{-1}$and 2853 cm^{-1} attributed to the C-H groups, and the quaternary ammonium group signals are detected at 1466 $cm^{-1}$and 1377 cm^{-1}[35, 36] (**Fig. 1a**). The broad characteristic peak of -OH groups at 3373 cm^{-1} indicates the presence of some trapped moisture within the Aliquat 336 sample [35]. The FTIR spectrum of 2NPOE exhibits two bands at 2924 cm^{-1} and 2855 cm^{-1}attributed to phenol and aliphatic C-H groups (**Fig. 1a**). The -NO_2 group is characterized by the band at 1522 cm^{-1}, the C-N group is detected at 1350 cm^{-1}, and the bands between 1020 cm^{-1} and 1170 cm^{-1} attributed to the C-O-C group and the C-H groups are detected at 740 cm^{-1} [22, 37]. For the pristine PVDF membrane, the two absorption bands at 1166 cm^{-1} and 1230 cm^{-1} are associated with the -CF_2- group of the PVDF main chain and the band located at 1401 cm^{-1} is attributed to the C–F group [38, 39].

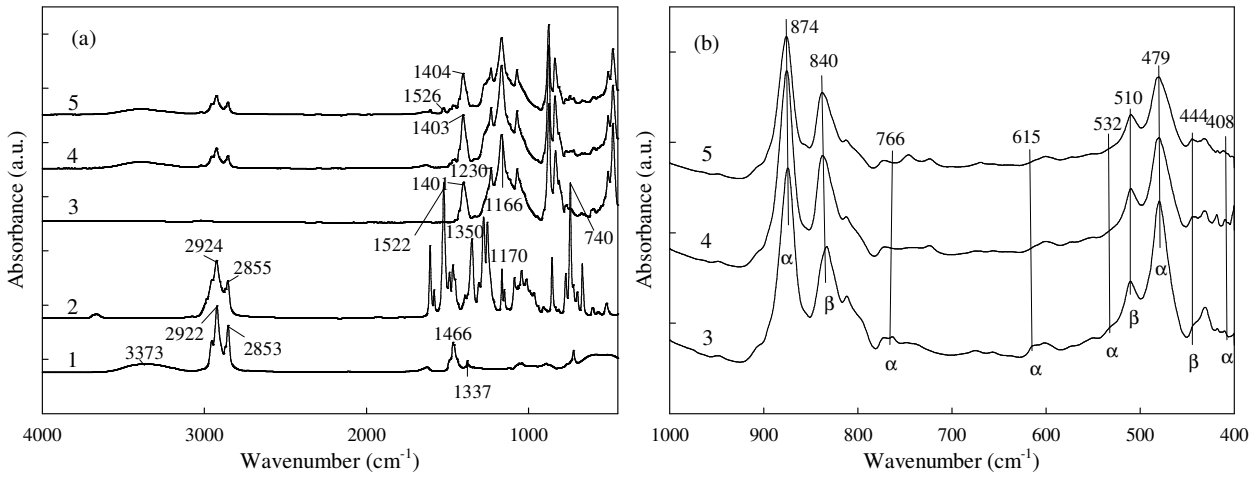

Fig. 1. FTIR spectra of the different membrane components and PIMs: (*1*) Aliquat 336, (*2*) 2NPOE, (*3*) PVDF, (*4*) 80PVDF/20Aliquat336, (*5*) 75PVDF/20Aliquat 336/5-2NPOE: (a) whole studied wavenumber region; (b) zoom of the wavenumber region for PIMs.

It is known that one of the attractive characteristics of PVDF is its polymorphism, i.e. the possibility to form different crystalline structures, and depending on the crystallization conditions PVDF may present at least four different crystalline structures: the orthorhombic α, β and δ phases and the monoclinic γ phase. Besides, the crystalline phases of PVDF can be characterized by the infrared absorption bands between 400 $cm^{-1}$and 1000 cm^{-1} [40] (**Fig. 1b**). The amorphous phase is characterized by two bands at 479 cm^{-1} and 874 cm^{-1} [40, 41]. The low intensity bands at 408 cm^{-1}, 532 cm^{-1}, 615 cm^{-1} and 766 cm^{-1} are attributed to the α phase of PVDF, the more pronounced bands at 444 cm^{-1}, 510 cm^{-1} and 840cm^{-1} are related to the β phase. This result proves the domination of the β phase in the elaborated PVDF membrane.

In order to quantify the β phase content $F(\beta)$ in PVDF-based membranes the following equation was used [34, 42]:

$$F(\beta) = \frac{A_\beta}{(K_\beta / K_\alpha)A_\alpha + A_\beta}, \quad (7)$$

where A_α and A_β represent the absorbance at 766 cm^{-1} and 840 cm^{-1} corresponding to the α and β phases, respectively; K_α and K_β are the absorption coefficients at the respective wavenumber equal to $6.1 \cdot 10^4$ and $7.7 \cdot 10^4$ cm^2/mol, respectively. The β phase content is estimated to be 80.6% for pure PVDF membrane. This result is in good agreement with the result found by Ferreira et al. for PVDF membrane prepared by the solvent evaporation method using DMF as a solvent, exactly $F(\beta)$ was found to be 65-80% depending on the polymer weight content and the solvent evaporation temperature [34].

The spectra of the 80PVDF/20Aliquat 336 and 75PVDF/20Aliquat 336/5-2NPOE membranes do not reveal the appearance of new peaks associated to new absorption bands (**Fig. 1**). This fact indicates that there are no covalent bonds between the membrane components. This result allows us to suppose that only weak interactions (such as van der Waals or hydrogen bonds) exist between the PIM components and that the liquid compounds (i.e. Aliquat 336 and 2NPOE) are physically immobilized in the PVDF matrix. However, the band at 1401 cm^{-1} which corresponds to the C-F group in pure PVDF is shifted to 1403 cm^{-1} and 1404 cm^{-1} for 80PVDF/20Aliquat 336 and 75PVDF/20Aliquat 336/5-2NPOE, respectively (**Fig. 1a**). Such slight shift towards higher wavenumber indicates possible intermolecular interactions of membrane different components, thus intermolecular interactions between the C-F negatively charged groups of PVDF and the positively charged ammonium group of Aliquat 336 exist. The similar result was already found in PIMs based on CTA [13, 21]. The shift of the band corresponding to the -NO_2 group from 1522 cm^{-1} in pure

2NPOE to 1526 cm^{-1} in 75PVDF/20Aliquat 336/5-2NPOEis also observed, suggesting intermolecular interactions between the -NO_2 group of 2NPOE and the ammonium group of Aliquat 336.

As to the PVDF crystalline phase, it is not changed significantly in case of PVDF-based PIMs. And really, in both PIMs (i.e. 80PVDF/20Aliquat 336 and 75PVDF/20Aliquat 336/5-2NPOE) the β phase is dominant with the *F(β)* content of 83.1% for the 80PVDF/20Aliquat 336 membrane and 82.0% for the 75PVDF/20Aliquat 336/5-2NPOE membrane. The observed slight difference in the *F(β)* content for PIMs compared to the pure PVDF membrane (*F(β)* = 80.6%) can be attributed to the ability of the ionic liquid to favour the formation of the β phase [43].

3.1.2. Mechanical performance

Mechanical resistance is one of the key factors for the membrane use as PIM should be flexible and able to be applied in transport modules, i.e. PIM should possess low Young's modulus value, and rather high elongation at break and tensile strength values. To study the influence of the ionic liquid and plasticizer presence on the mechanical behaviour of the PVDF-based membranes, tensile tests were carried out. The stress-strain curves of the pure PVDF and blend membranes are shown in **Fig. 2a**. The average values of the Young's modulus, tensile strength and elongation at break determined from these curves are gathered in **Table 1**. As one can see, pure PVDF has a Young's modulus of about 1877 MPa, that agrees well with the values found in literature for the PVDF membranes prepared using acetone and DMF as solvents [34,

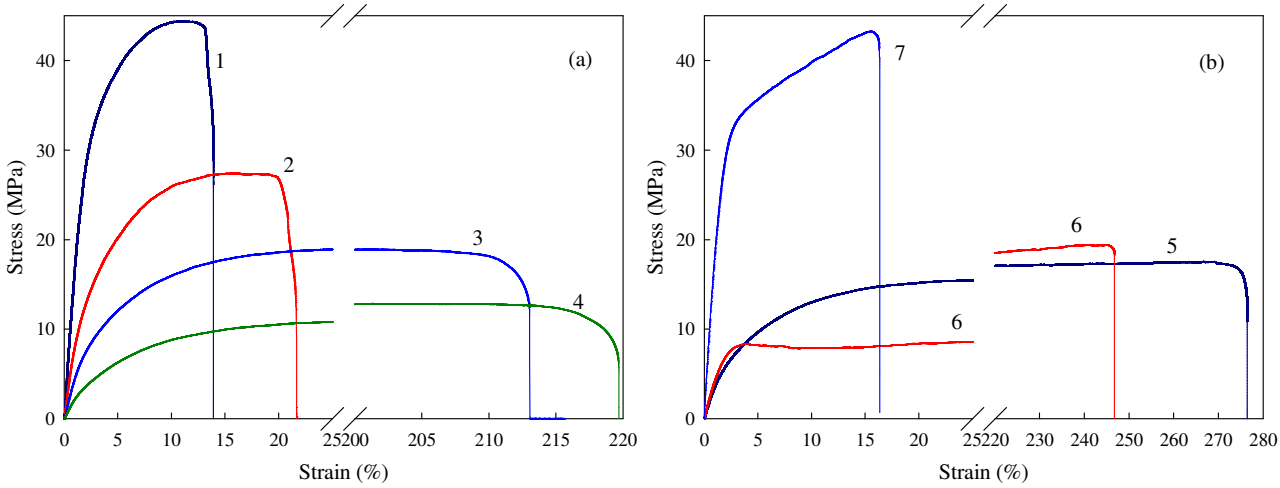

Fig. 2. Stress-strain curves of PVDF-based PIMs (*a*) and PIMs based on different polymers (*b*): (*1*) PVDF, (*2*) 90PVDF/10Aliquat 336, (*3*) 80PVDF/20Aliquat 336,

(*4*) 70PVDF/30Aliquat 336, (*5*) 75PVDF/20Aliquat 336/5-2NPOE,
(*6*) 75PVC/20Aliquat 336/5-2NPOE, (*7*) 75CTA/20Aliquat 336/5-2NPOE.

44, 45]. It should be mentioned that the mechanical properties of the PVDF membrane depend strongly on the PVDF solubilization step, the used ratio of the solvent/polymer and the solvent evaporation temperature [34, 45].

The plasticizing effect of Aliquat 336 on the behaviour of some polymers, such as PVC and CTA, has been already reported in literature [13, 46]. And really, the addition of the ionic liquid and plasticizer in the PVDF membrane modifies significantly membrane mechanical properties. For example, with 20% of Aliquat 336 in the membrane, the Young's modulus decreases from 1877 MPa to 487 MPa (**Fig. 2a** and **Table 1**). The tensile strength value is also reduced from ~42 MPa to ~12MPa for the pure PVDF and 70PVDF/30Aliquat 336 membranes, respectively (**Table 1**). This decrease in tensile strength is accompanied by a high increase of elongation at break – from 12% for the pure PVDF membrane to 187% for the 70PVDF/30Aliquat 336 membrane. This fact confirms the plasticizing effect observed in case of the ionic liquid presence in membranes. Further addition of 5% of plasticizer (2NPOE) almost doubles the elongation at break values (**Table 1**). Moreover, the stiffness is reduced and the flexibility increased, thus promoting elongation at break and, therefore, such membranes can be used in aqueous media without any risk of tearing. The similar effect is observed for the PVDF-based membranes with other ionic liquids [42, 43].

Table 1. Mechanical behaviour of different studied PIMs.

Membrane	Young's modulus (MPa)	Tensile strength (MPa)	Elongation at break (%)
PVDF	1877 ± 73	42.0 ± 1.2	12.4 ± 1.4
90PVDF/10Aliquat336	922 ± 71	26.1 ± 1.9	20.6 ± 3.6
80PVDF/20Aliquat336	487 ± 33	16.8 ± 1.8	184.3 ± 56.6
70PVDF/30Aliquat336	250 ± 12	12.2 ± 1.9	187.2 ± 62.2
75PVDF/20Aliquat336/5-2NPOE	414 ± 13	15.9 ± 2.2	238.9 ± 82.6
75PVC/20Aliquat336/5-2NPOE	496 ± 54	17.8 ± 2.0	212.9 ± 45.5
75CTA/20Aliquat336/5-2NPOE	2023 ± 58	40.8 ± 6.3	13.9 ± 2.4

In order to investigate the effect of the polymer matrix on the elastic behavior of the membranes, the mechanical properties of PVDF-based PIMs were compared to the behaviour of PVC- and CTA-based PIMs which are widely used in the studies of the metal ions transport. All membranes contain the same quantity of ion carrier (i.e. Aliquat 336) (20%) and plasticizer (2NPOE) (5%). The tensile behavior of PIMs based on CTA, PVC and PVDF is presented in **Fig. 2b** and the values of Young's modulus, stress at break, and elongation at break are given in **Table 1**. According to these data, PVDF- and PVC-based PIMs have rather similar mechanical properties, whereas CTA-based PIM is much more resistant. The Young's modulus of CTA-based PIM is four to five times higher than that of the membranes based on PVC and PVDF. Compared to PVC- and PVDF-based PIMs, the elongation at break value is reduced by 20 times and the strength at break value is almost 3 times higher for CTA-based PIM. This result agrees well with literature as the higher mechanical resistance of CTA-based PIM compared to PVC-based PIMs is revealed [46, 47].

3.1.3. Hydrophobic/hydrophilic character

The water contact angle measurements were performed in order to estimate the membrane wettability as the hydrophilic/hydrophobic balance is a decisive parameter for the transport performance and stability of PIMs. The membrane hydrophilic nature is favorable for the membrane wettability as the hydration process will be fast in this case. However, the hydrophobic behavior assures the membrane stability as it will delay the carrier leakage.

Pure PVDF is known for its hydrophobic character [24]. However, the hydrophobicity of the PVDF membrane surface can be modified during the preparation step [23, 24]. In order to determine the wettability character of membrane surfaces, the water contact angle measurements were performed. The variation of water contact angle values for different prepared PIMs is shown in **Fig. 3**. The pure PVDF membrane reveals the water contact angle value around 71°. Besides, this value is almost constant up to 3 min of measurements. The obtained value is close to values found in literature for the dense PVDF membranes elaborated with DMF [41, 48].

The addition of Aliquat 336 to the membrane increases strongly the membrane hydrophilicity (**Fig. 3a**). For example, the membrane containing 10% of Aliquat 336 has the same contact angle value as the pure PVDF membrane at $t = 0$. However, this value decreases up to 33° after 180s of the water drop deposition. When the Aliquat 336 content in the PVDF matrix exceeds 10%, the water contact angle dramatically is reduced and it is ~26° at $t = 0$ and slows down to ~10° after 180s for the PVDF-based membranes containing 20% and 30%

Aliquat 336. Thus, the character of PVDF-based PIMs turns from a slightly hydrophilic to a very pronounced hydrophilic one. This behaviour is also observed for the membranes based on CTA and PVC [46] and can be explained by the presence of the quaternary ammonium group of Aliquat 336 known by its hydrophilic property. Therefore, one can conclude that the functional group is turned to the membrane surface [47]. Further addition of plasticizer (i.e. 5% of 2NPOE) induces a small increase of hydrophobicity due to the presence of the hydrophobic alkyl chain of 2NPOE (**Fig. 3a**).

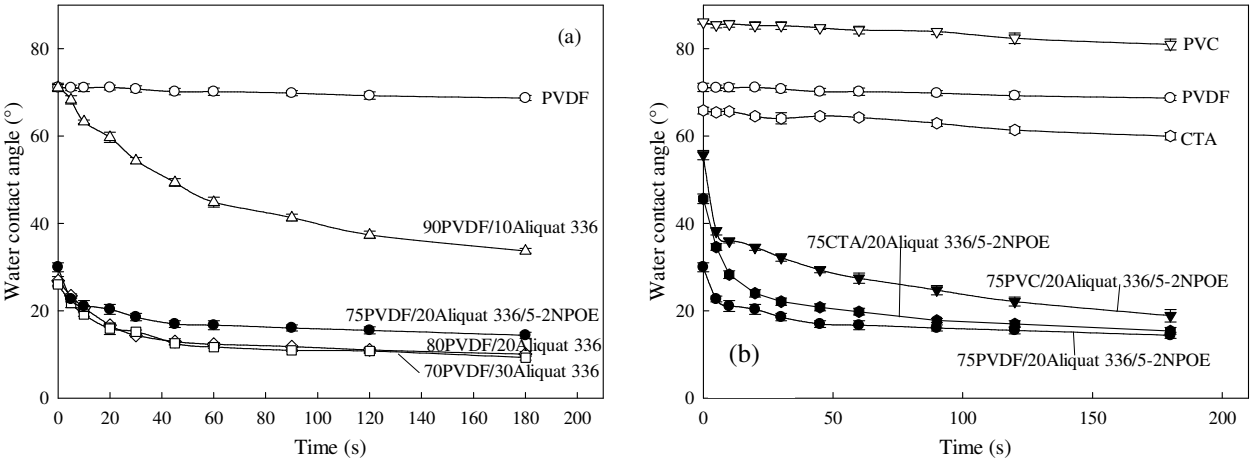

Fig. 3. Water contact angle variation as a function of the deposition time for PVDF-based PIMs (*a*) and PIMs based on different polymers (*b*).
Open symbols correspond to the pure polymer membrane, filled symbols correspond to PIM.

In order to study the influence of the polymer matrix on the PIMs wettability, the measurements for PVC- and CTA-based PIMs were also carried out (**Fig. 3b**). As expected, the pure CTA membrane is the most hydrophilic one. As it was already reported in literature, CTA-based PIM is more hydrophilic than PVC-based one if the amount of Aliquat 336 is rather low and does not exceed 40% [46]. However, in our case, PVDF-based PIM is the most hydrophilic among three studied PIMs despite the slightly more hydrophilic character of CTA compared to PVDF (**Fig. 3b**). This result may be explained by the homogeneous distribution and saturation of the PVDF surface with only 20% of Aliquat 336 (as the water contact angle does not vary for PIMs with 20 and 30% of Aliquat 336 as shown in **Fig. 3a**) as compared with PVC- and CTA-based PIMs for which at least 40% of Aliquat 336 is required for the surface saturation [46]. According to the reported results [21, 47, 49], the membrane hydrophilic character is a determining factor for the transport properties of the metal ions

391 through PIMs. So, the improved Cr(VI) transport performance is expected for the elaborated
392 75PVDF/20Aliquat 336/5-2NPOE membrane compared to the CTA- and PVC-based PIMs.
393
394
395 **3.1.4. Membrane morphology**
396 One of the PIM important characteristics is the membrane microstructure as it allows
397 us to control the carrier distribution and it affects the membrane transport efficiency.
398 Moreover, the morphology and the structure of the PVDF-based membranes depend strongly
399 on the preparation method. For example, the phase inversion technique by immersion in the
400 non-solvent allows obtaining the membranes with an asymmetric porous structure that
401 weakens the membrane mechanical properties [26, 27, 32, 34]. Moreover, the use of this
402 technique for the PIM elaboration leads to the ion carrier loss during the step of the
403 immersion in the non-solvent (i.e. water) [28]. So, in order to obtain dense and, thus,
404 mechanically resistant PIMs the solvent evaporation technique is preferably used.
405 As one can see from the obtained SEM images (**Fig. 4**), the membrane surface in
406 contact with the glass plate is dense and smooth, while the membrane surface in contact with
407 air presents a granular structure with some pores, whatever the membrane composition.
408 Similar results were reported for the pure PVDF membranes casted from different solvents
409 [40] as well as for the PVDF membranes with 1-butyl-3-methylimidazolium
410 bis(trifluoromethylsulfonyl)imide [43]. In fact, the solid/liquid phase separation during the
411 solvent evaporation leads to the formation of the crystalline phase in the membrane.
412 Therefore, spherulites are formed, and the membrane presents the spherulite porous structure
413 [40, 43]. Besides, the presence of Aliquat 336 in the PVDF membrane allows obtaining more
414 porous structure as compared with the pure PVDF membrane. Moreover, the addition of 5%
415 of 2NPOE leads to the higher membrane porosity (**Fig. 4**). It should be also mentioned that if
416 the glass contacting surfaces in the PVDF and PVDF/Aliquat 336 membranes are perfectly
417 smooth, the surface becomes slightly rough in the presence of 2NPOE. The growth of
418 spherulites and the addition of 2NPOE ensure the higher membrane roughness and promote
419 the formation of surface pores, thus providing a greater interfacial surface area and improving
420 the metal ion extraction and transport [27, 28].
421 The SEM cross section images of all membranes reveal homogeneous and dense
422 structure without macro-voids (**Fig. 4**), meaning that the pores present on the membrane
423 surface are not interpenetrated. The obtained results testify to the good compatibility of
424 membranes compounds (i.e. PVDF, Aliquat 336 and 2NPOE).

425

426

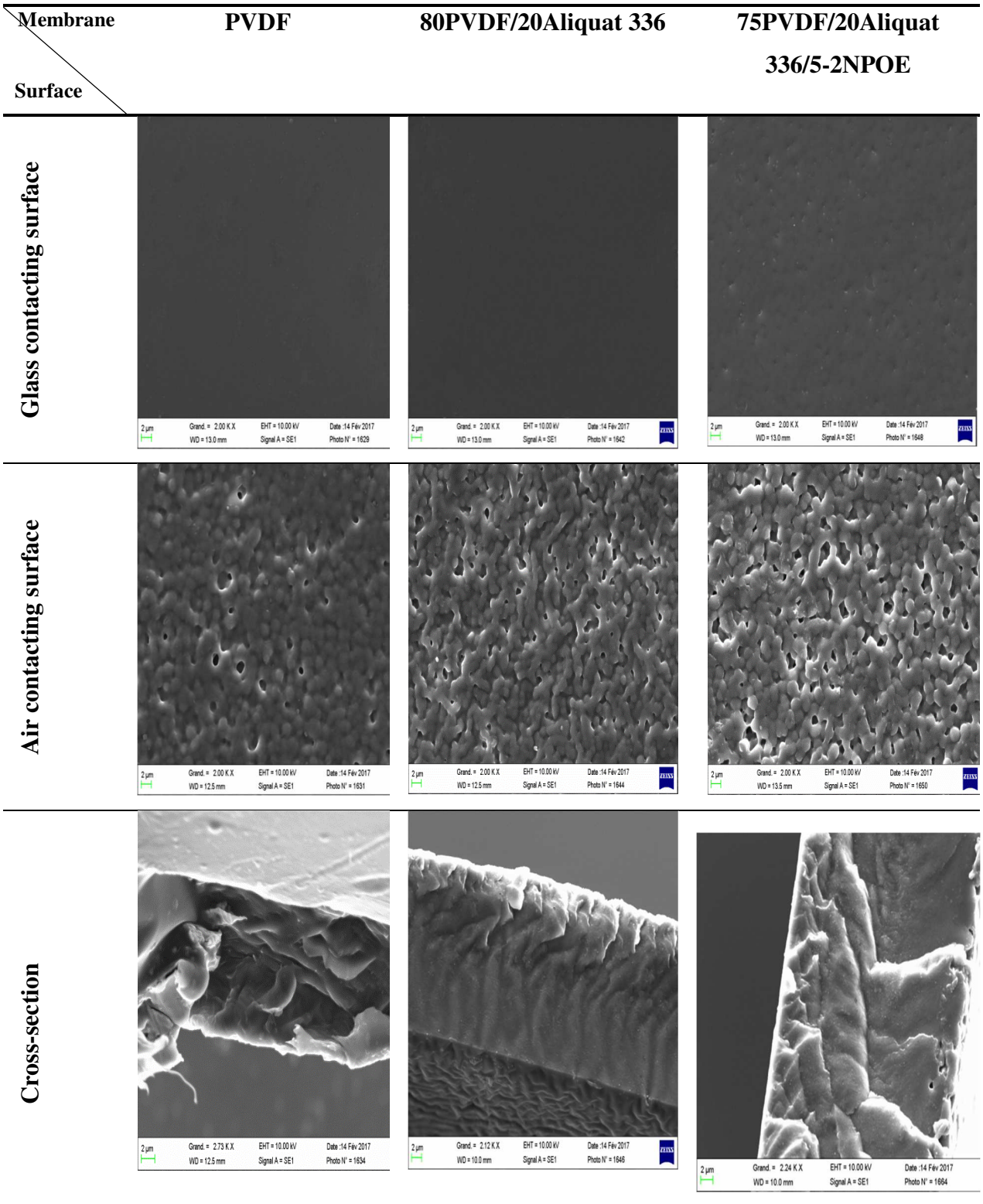

427

428 **Fig. 4.** SEM images of different PVDF-based membranes.

3.1.5. Thermal properties

It was shown that imidazolium-based ionic liquids modified the PVDF crystallization kinetic and slowed down the growth of the crystalline phase [42, 43]. So, DSC measurements were carried out in order to analyze the eventual variations in the PIM phase transitions during the incorporation of the ionic liquid and plasticizer and also in order to detect probable interactions between the three constituents of the membrane, i.e. polymer, ion carrier and plasticizer. Besides, as the crystals allowed to increase the tortuosity pathways for the ion transport, so it is important to quantify the membrane microstructure (i.e. amorphous and crystalline domains). The PVDF crystallinity degree $X_{c(\mathrm{PVDF})}$ was estimated according to the following equation [40, 43] taking into account the polymer weight proportion:

$$\chi_{c(\mathrm{PVDF})} = \frac{\Delta H}{\Delta H_m (1-\phi)} \ , \qquad (8)$$

where ΔH and ΔH_m are the melting enthalpy of PVDF-based PIM and 100% crystalline PVDF, respectively. ϕ is the total mass fraction of Aliquat 336 and NPOE in PIM. The value of ΔH_m has been estimated to be 104.7 J/g [43]. The total membrane crystallinity degree X_c was determined from Eq. 8 with $\phi = 0$.

The melting temperature and enthalpy as well as crystallinity degree for PVDF-based PIMs are summarized in **Table 2**. The endothermic peak at 164.7°C present on the DSC curve of pure PVDF (not shown) corresponds to the melting temperature T_m of the crystalline phase. The melting point depression (i.e. the shift of the T_m value to the lower temperatures) is observed for PVDF-based PIMs. Such decrease may be attributed to the strong electrostatic interactions between the ionic liquid (Aliquat 336) and the crystalline phase of polymer that leads to lower cohesive energy of the crystalline phase and, so, a lower thermal energy is sufficient for the crystalline phase melting [42]. This decrease of T_m also indicates that the crystal growth is affected by interactions between the membrane liquid compounds (i.e. Aliquat 336 and 2NPOE) and the PVDF chains. This fact testifies to a compatibility of the PVDF base polymer and the membrane liquid components.

It can be seen that the incorporation of Aliquat 336 in PIMs leads to the decrease of the membrane crystallinity degree. Such behaviour has been already observed for the PVDF membranes with other ionic liquids [42-44]. A slight increase of the crystallinity degree is noted for the membrane containing 20% of Aliquat 336 and 5% of 2NPOE, which may be explained by the fact that the plasticizer (2NPOE) enhances the PVDF chain segment mobility

necessary for crystallization. The increase of the amorphous phase in PIMs can be favorable for the extraction of the metal ions as the transport occurs usually in the non-crystalline zones [13].

Table 2. Thermal characteristics of PVDF-based PIMs.

Membrane	Melting temperature (°C)	Melting enthalpy ΔH_m (mJ/mg)	Crystallinity degree (%)	
			$X_{c(PVDF)}$	X_c
PVDF	164.7	53.9	51.5	-
90PVDF/10Aliquat336	164.4	31.5	33.4	30.1
80PVDF/20Aliquat336	158.2	28.1	33.6	26.9
70PVDF/30Aliquat336	157.0	28.8	39.3	27.5
75PVDF/20Aliquat336/5-2NPOE	159.2	33.8	43.1	32.3

Thermogravimetric analysis (TGA) was performed in order to study the thermal stability of the elaborated membranes. The obtained TGA curves are presented in **Fig. 5a**. For the sake of clarity, the thermogravimetrical derivative curves (DTG) are also shown (**Fig. 5b**).

As one can see from TGA thermogram of Aliquat 336, the weight loss is observed from the beginning of the heating that can be linked to the presence of certain moisture within the ionic liquid. This fact confirms the FTIR result, where a bonded -OH peak is recorded **(Fig. 1a)**. The trapped moisture alters significantly the stability of ionic liquids [50]. The onset degradation of Aliquat 336 is about 160°C and it decomposes completely at about 240°C just after its boiling point (i.e. 225°C). 2NPOE begins to decompose a little bit before Aliquat 336 – at ~150°C as its boiling point (198°C) is lower than that of Aliquat 336. The pure PVDF membrane is characterized by a single degradation step at 450°C associated with the breaking of C-H and C-F bonds and the formation of C=C bond [42]. After the Aliquat 336 introduction into PVDF, the thermal behaviour of PVDF-based PIM is changed as two degradation steps are noted: the first one starts at 170°C and corresponds to the Aliquat 336 degradation and the second one observed at 430°C relates to the degradation of the PVDF skeleton. Besides, the incorporation of Aliquat 336 into the PVDF matrix delays the Aliquat 336 degradation probably due to its possible interactions with the PVDF chains. The membrane containing Aliquat 336 and 2NPOE also degrades in two stages: at 160°C the degradation of Aliquat 336 and 2NPOE is noted and at 430°C the PVDF decomposition is

observed. In this case, the decomposition of Aliquat 336 and 2NPOE occurs at the same temperature. Besides, it is found that due to the interactions between 2NPOE and CTA, the 2NPOE decomposition is observed at temperature higher than its boiling temperature [37, 47]. One can note that the PVDF degradation temperature in PVDF-based PIMs is also shifted towards higher temperatures as compared with its degradation in individual state (**Fig. 5b**), thus confirming the PVDF interactions with the membrane liquid compounds, i.e. ion carrier and plasticizer.

3.2. Transport study of PVDF-based PIMs

Due to its hydrophilic character, high flexibility and surface roughness, the 75PVDF/20Aliquat 336/5-2NPOE membrane should be efficient for the Cr(VI) removal. In order to verify this supposition, all elaborated membranes were tested for the Cr(VI) transport in the acid medium. For the results reproducibility, the tests were repeated at least three times

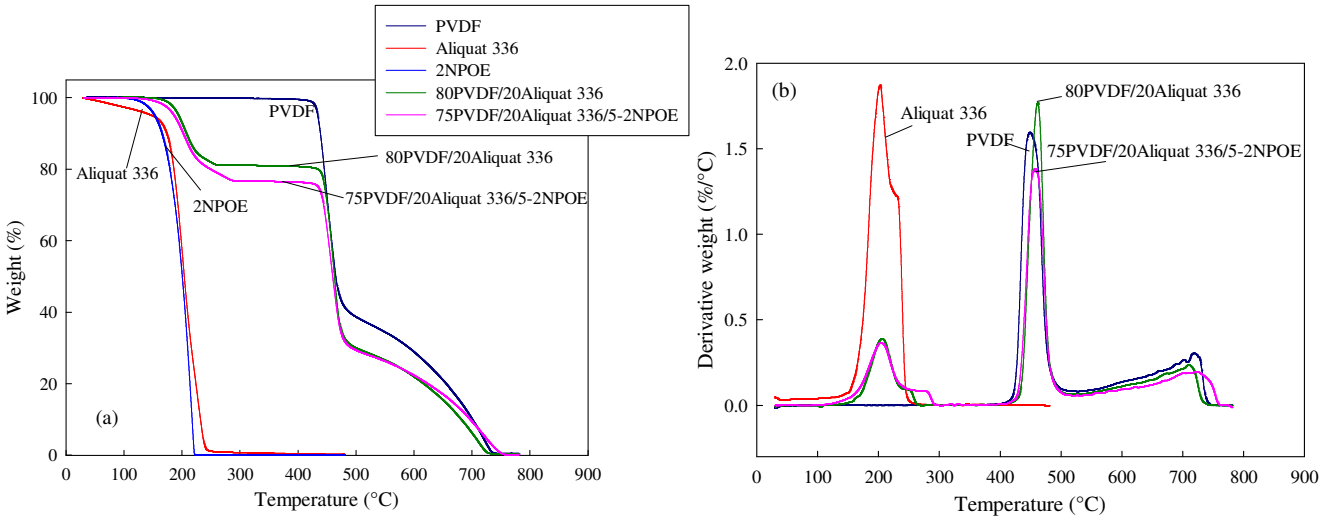

Fig. 5. Thermogravimetric (*a*) and DTG (*b*) curves of studied materials.

for the membranes prepared from the same casting solution as well as for the membranes prepared with the other casting solution.

Prior to measurements of PVDF-based PIMs, the pure PVDF membrane and the PVDF membrane containing only the plasticizer (i.e. 2NPOE) were tested. In the absence of the ion carrier, no transport from the donor to acceptor phase was detected. This result allows us to conclude that the membrane without the ion carrier serves as a barrier to the metal ion permeation.

3.2.1. Effect of the stripping phase composition

Cr(VI) ions are transported into the membrane from the donor phase to the acceptor phase by the diffusion phenomenon under the effect of a driving force created by the gradient of chemical potential between these two phases [13, 25, 30, 51]. In general, the donor phase consists of Cr(VI) ions diluted in hydrochloric acid or sulphuric acid, and the acceptor phase is an alkaline medium – often NaOH solution [21, 25, 30, 52]. The evolution of the Cr(VI) concentration in the source and receptor phases as a function of time for different stripping phase composition is shown in **Fig. 6**. As one can see, the decrease of the Cr(VI) concentration in the source phase is accompanied by an increase of its concentration in the receiving phase indicating that the metal ions are successfully transported from the source to receptor phase with a removal factor > 99%. However, when the receiving medium consists of 0.1M NaOH, the membrane changes its color and in some time (after one cycle, i.e. 12h) becomes black (see insert to **Fig. 6a**). Besides, it is fragile and brittle at the end of the experiment, thus preventing its reuse for further transport cycles. The PVDF chemical stability in the acidic medium can be

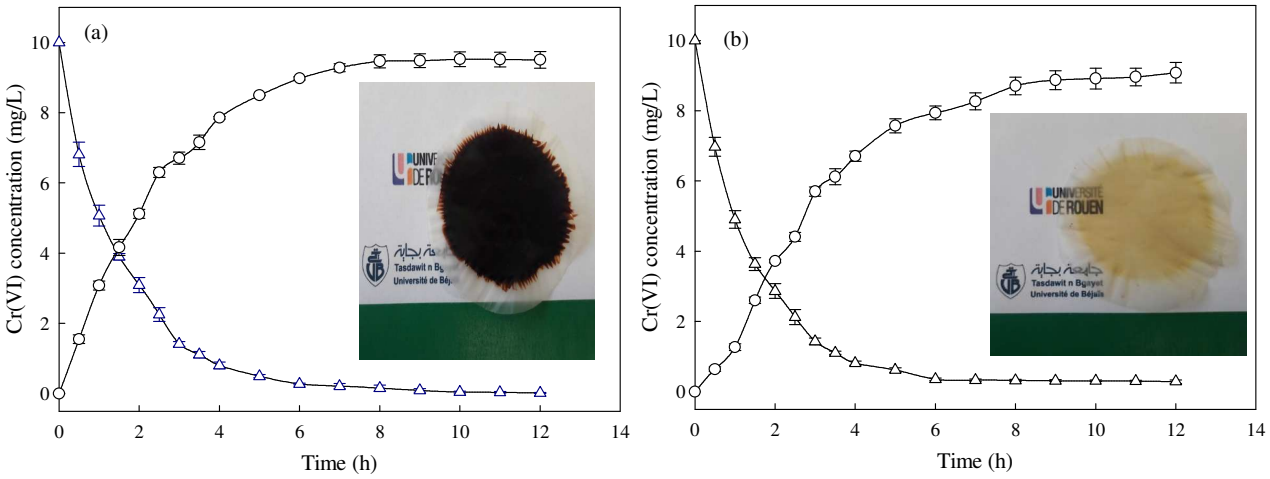

Fig. 6. Transient concentration curves of the Cr(VI) transport through the 70PVDF/30Aliquat 336 membrane for the feed (*Δ*) and receiving (*o*) phases for different stripping solutions: *(a)* 0.1 M NaOH solution, (*b*) acetic acid/ammonium acetate (pH 5) solution. Insert: the photo of PIM after 1 cycle of use (12h).

considered as excellent [23, 38, 39]. However, numerous studies reported the observed color changing of PVDF from white to brown and finally to black upon the immersion into NaOH solution as PVDF is chemically attacked by alkaline solutions [23, 27], therefore, the PVDF reuse and stability are affected. That's why in order to ensure the membrane stability and

possibility for reusing, the acceptor phase was buffered at pH 5 by using an acetic acid/ammonium acetate buffer solution. This solution has been already effectively used for the Cr(VI) back extraction [51, 53]. As shown in **Fig. 6b**, the recovery factor of ~90% is obtained during the Cr(VI) extraction in the buffer medium. Moreover, the use of acetic acid/ammonium acetate buffer solution makes it possible to keep the membrane in its initial state as no deterioration can be seen (see insert to **Fig. 6b**). However, some quantity of Cr(VI) is accumulated inside the membrane at the end of the experiment giving a yellow color to the membrane.

So, the acetic acid/ammonium acetate buffer solution (pH 5) makes it possible to avoid the chemical deterioration of the PVDF membrane and, thus, this solution is used as a receptor phase for further study. Since Cr(VI) is well separated by the elaborated membranes and, thus, the Cr(VI) concentration becomes high enough in the receiving phase, it later can be reused in another cycle in chemical industry. Also, the Cr(VI) ions can be recuperated by their precipitation after the reduction into the cationic form of Cr(III) [19, 52].

3.2.2. Optimization of the membrane composition and the Cr(VI) concentration effect

In order to determine the influence of the ion carrier content on the membrane transport efficiency, PIMs with different Aliquat 336 concentration ranging from 0% to 30% were tested for the Cr(VI) removal during 12h (**Fig. 7a**). As one can see, the membrane without the carrier (i.e. pure PVDF) did not remove Cr(VI). This result confirms that the ionic liquid (Aliquat 336) acts as an ion carrier. Besides, the membrane with only 10% of Aliquat 336 does not transport Cr(VI) ions into the acceptor phase and the extracted chromium is accumulated inside the membrane testifying that the carrier concentration is below the percolation threshold limit [52].

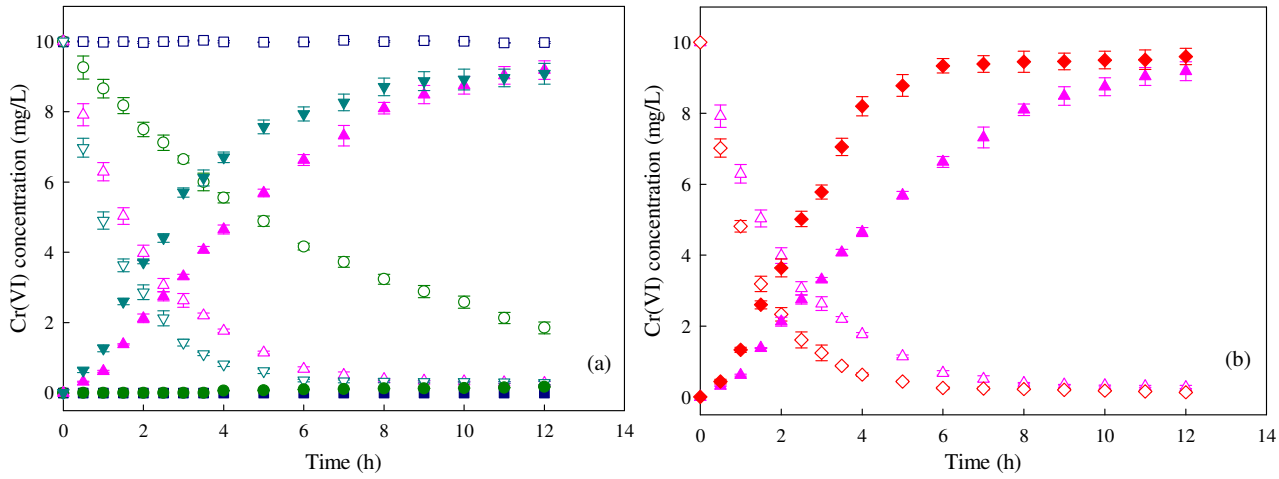

Fig. 7. Transient Cr(VI) concentration curves for the feed (open symbols) and stripping (filled symbols) phases for different membranes: (□)PVDF, (*o*) 90PVDF/10Aliquat 336, (*Δ*) 80PVDF/20Aliquat 336, (▽)70PVDF/30Aliquat 336, (◊) 75PVDF/20Aliquat 336/5-2NPOE:

(*a*) influence of the Aliquat 336 concentration, (*b*) influence of the 2NPOE presence.

In the case of the PVDF-based membranes with the Aliquat 336 concentration above the percolation threshold (i.e. above 10%), a gradual increase of the extraction percentage (both removal and recovery factors) and of the flux is observed (**Table 3**). This result indicates that the presence in PVDF-based PIM of only 20% of Aliquat 336 is sufficient to ensure the complete removal of Cr(VI) ions from the donor phase. The increase of the Aliquat 336 concentration to 30% induces only the transport flux increase. It should be mentioned that in case of traditional PIMs (i.e. based on PVC and CTA), in order to ensure the effective Cr(VI) transport more than 20% of Aliquat 336 (in some cases even more than 40%) or more than 30% of plasticizers must be incorporated into the membrane [21, 52]. At the end of the experiment the membrane became yellow (see insert to **Fig. 6b**) due to the accumulation of some quantity of Cr(VI) (about 10%) in the membrane phase.

Table 3. Cr(VI) transport performance of the PVDF-based PIMs.

Membrane	Flux (µmol/(cm²·s))	Removal factor (%)	Recovery factor (%)
90PVDF/10Aliquat336	/	80.5 ± 2.0	1.7 ± 0.1
80PVDF/20Aliquat336	3.8 ± 0.1	97.2 ± 0.3	92.5 ± 2.5

70PVDF/30Aliquat336	5.0 ± 0.2	97.0 ± 0.3	90.7 ± 2.1

It is known that the addition of plasticizer can improve the permeability properties of PIMs by enhancing the compatibility of the membrane components [7, 53]. Therefore, the effect of the 2NPOE addition on the membrane permeability properties was examined (**Fig. 7b**). As one can see from the obtained results, the plasticizer improves the back extraction of Cr(VI) (recovery factor > 95%). At the same time, the equilibrium time is reduced and the transport flux is enhanced from 3.8 µmol/(m²·s) for 80PVDF/20Aliquat 336 to 5.6 µmol/(m²·s) for PIM containing only 5% of 2NPOE. This result can be explained by the fact that the plasticizing action of 2NPOE improves the Cr(VI) ions mobility [21] as both membranes have practically the same content of the crystalline phase fraction (~30%, **Table 2**). Turgut et al. studied the influence of 2NPOE on the Cr(VI) transport using PVDF-*co*-HFP and imidazolium bromide room temperature ionic liquid [30]. They found that the addition of about 6% of 2NPOE modified the PIM structure by creating more pores on the surface and increasing its roughness, thus significantly improving the transport flux as a larger interfacial surface was created.

Also, the influence of the Cr(VI) initial concentration on the transport flux was investigated. It was revealed that the increase of the transport flux was observed with the Cr(VI) concentration increase. Besides, this dependency was linear. For example, for the donor phase containing 10 mg/L of Cr(VI) the flux of 5.58 ± 0.20 µmol/(m^2·s) was observed, whereas the flux was 12.28 ± 0.30 µmol/(m^2·s) when the concentration became four time higher, i.e. 40 mg/L. These experimental results are in good agreement with Eq. 3.

3.2.3. Effect of polymer matrix

In order to study the effect of the polymer matrix on the Cr(VI) transport properties, the performance of PVDF-based PIM containing 20% of Aliquat 336 and 5% of 2NPOE was compared with the behaviour of membranes containing the same amount of the ion carrier and plasticizer and based on CTA and PVC. It has been already shown that CTA-based PIMs are more efficient than PVC-based PIMs during facilitated transport of chromate ions [21, 49] and $Ag(CN)_2^-$ ions [47], especially when a small amount of the ion carrier is incorporated in the polymer matrix due to the more hydrophilic nature of CTA. The evolution of the Cr(VI) concentration in the feed and receiving phases is shown in **Fig. 8** for PIMs based on three studied polymers. As it can be seen, PVDF-based PIM is the most efficient as more than 98%

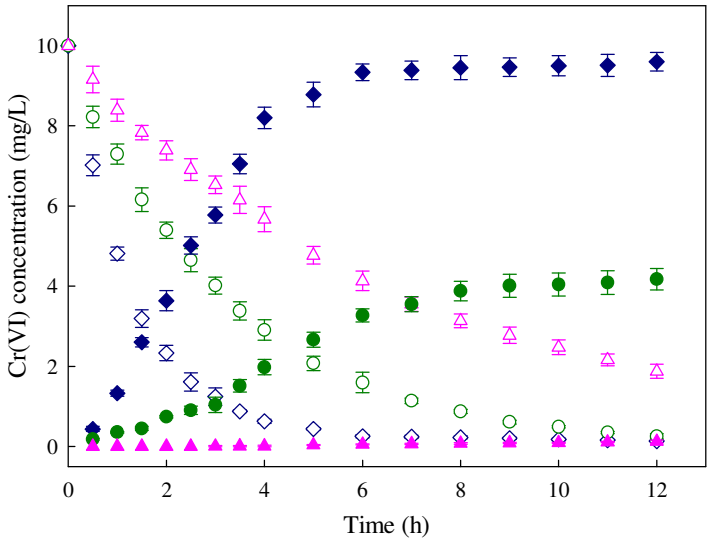

Fig. 8. Effect of the polymer matrix on the Cr(VI) transport properties for the feed (open symbols) and stripping (filled symbols) phases: (◊) 75PVDF/20Aliquat 336/5-2NPOE; (Δ)75PVC/20Aliquat 336/5-2NPOE; (o)75CTA/20Aliquat 336/5-2NPOE.

of Cr(VI) is removed in only 6h with a back extraction factor higher than 95% and the transport flux of 5.6 µmol/(m^2·s).The efficiency of CTA-based PIM is lower than that of PVDF-based PIM. In this case, the removal factor of 97% of Cr(VI) requires 12h of the transport experiment, the recovery factor is only 41%, and the transport flux equal to 2.6 µmol/(m^2·s), i.e. two times lower compared to the PVDF matrix, is obtained. In addition, no Cr(VI) transport was observed through PVC-based PIM (only 1.25% goes to the receiving phase), probably as in this case the ion carrier concentration was below the percolation threshold limit. After 12h of experiment, only 80% of Cr(VI) ions from the feed phase were removed by PVC-based PIM and were accumulated in the membrane.

One can conclude that with such a low concentration of the ion carrier and plasticizer (20% and 5%, respectively) the nature of the polymer matrix has a great influence on the PIM transport properties. Indeed, the use of CTA and PVC requires a higher amount of plasticizer to ensure the mobility of the target molecule complex and efficient facilitated transport [21, 22, 37, 47, 49, 53]. So, in our case only 5% of plasticizer incorporated into the CTA and PVC matrix can be insufficient to be efficient. According to the results of the mechanical traction tests (**Fig. 2b** and **Table 1**), PVC-based PIM is more plasticized compared to CTA-based PIM due to a higher plasticizing effect of Aliquat 336 on the PVC matrix [46, 47]. However, it seems to be that the membrane mechanical state is not the key parameter for the PIM

transport performance. In fact, the hydrophilic/hydrophobic character should be also taken into account. The higher efficiency in the Cr(VI) removal of CTA-based PIM can be explained by the higher hydrophilicity of CTA-based PIM compared to PVC-based PIM (**Fig. 3b**). As to PVDF-based PIM, its mechanical properties are close to those of PVC-based PIM (**Fig. 2b** and **Table 1**), it possesses the most hydrophilic character among three studied membranes (**Fig. 3b**), and its T_g is very low (about -39°C), meaning that the polymer is in its rubbery state characterized by the high polymer chains mobility. All these features promote the transfer of the molecule target/ion carrier complex even without a plasticizer. O'Bryan et al. reported that PVDF-*co*-HFP-based PIMs exhibited significantly higher rates of extraction and back extraction for SCN^- ions and long-term stability compared to PVC-based PIMs [28, 54].

3.2.4. Selectivity study

Generally, industrial activity generates effluents containing a mixture of heavy metal ions. Therefore, in addition to be effective and possess high permeability properties, PIM should be also selective in order to transport only specific species. In order to study the selectivity of PVDF-based PIMs towards Cr(VI) ions, the membrane with optimal composition, i.e. 75PVDF/20Aliquat 336/5-2NPOE, was used. A mixture solution containing Cr(VI), Co(II), Cu(II), Zn(II), Ni(II), Pb(II), Fe(III), Cd(II) with identical initial concentration of 10 mg/L was prepared in 0.1M HCl. The experiments were conducted for 8h. As one can see from the obtained results (**Fig. 9**), only Cr(VI) ions are transported with high efficiency (96.9%). Moreover, Co(II), Cu(II), Zn(II), Ni(II) and Pb(II) ions are not transported through this PIM. Cd(II) and Fe(III) may be transported at the same time with Cr(VI) but to a much less extent – 2.7% for Cd(II) ions and 0.3% for Fe(II) ions. The permeability of these ions may be explained by the formation of anionic complexes of Cd(II) and Fe(III) with Cl^- anions[30]. However, the quantity of these ions in the receiving phase remains negligible compared to the membrane recovery ability for Cr(VI) ions.

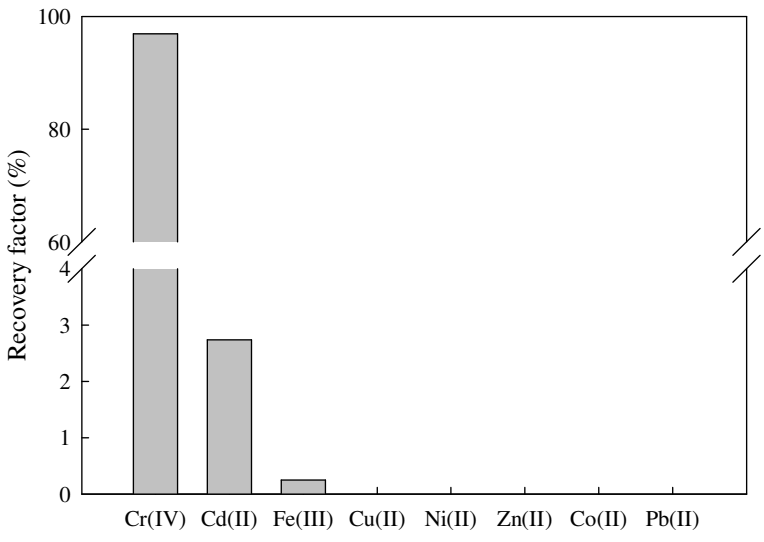

Fig. 9. Influence of the type of interfering ions on the Cr(VI) recovery capacity for 75PVDF/20Aliquat 336/5-2NPOE membrane.

3.2.5. PIM stability

In addition to the high transport efficiency, one of the most important parameters for large-scale application of PIM is its ability to be reused during several cycles without performance loss. Therefore, the stability of 75PVDF/20Aliquat 336/5-2NPOE PIM was evaluated on the basis of the recovery factor (Eq. 4) determined after 24 sequential cycles (1 cycle = 8h). These experiments were performed with the same membrane, while both the donor and acceptor phases were renewed after each cycle. The evolution of the recovery factor of the Cr(VI) transport is shown in **Fig. 10a**. No significant difference of the Cr(VI) recovery was observed during first 16 cycles (i.e. for 128h). During that time, the high recovery factor (~98%) remained constant. However, after this time a gradual decrease of the removal factor was

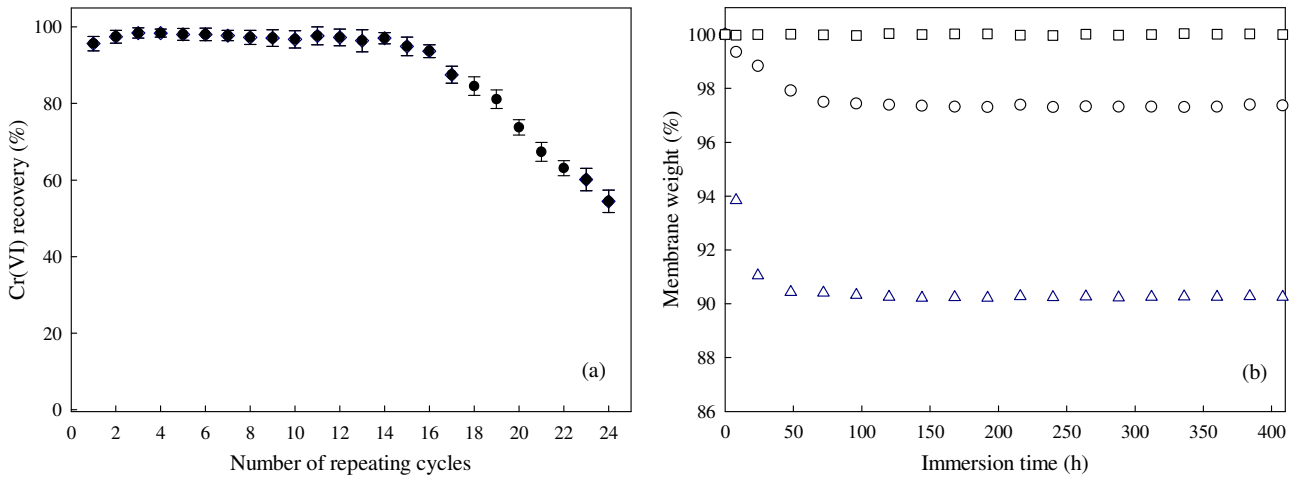

Fig. 10. (*a*) Recovery efficiency of 75PVDF/20Aliquat 336/5-2NPOE as a function of the number of measurements; (*b*) membrane weight as a function of the immersion time in

different solutions: (*Δ*) milli-Q water;(*o*) 0.1 MHCl; (□) buffer solution of acetic acid/ammonium acetate (pH 5).

observed – after 19 cycles (i.e. 152h) the recovery factor was reduced to ~81% and after 24 cycles (i.e. 192h) this value was 54%. This result testifies to the improvement of the recovery capacity and stability of the PVDF-based PIM compared to the membranes based on CTA and PVC [21, 53] and PVDF-*co*-HFP [28, 30]. This high stability of PVDF-based PIM can be explained by the reduced amount of liquid components (only 25%). The PVDF chemical stability and its resistance to hydrolysis and degradation also contribute to the improvement of the membrane performances and limitation of the liquid phase release. Moreover, the acceptor phase medium (i.e. buffer solution of acetic acid and ammonium acetate at pH 5) contributes to good membrane stability as it is shown that the NaOH solution usually used for the back extraction of Cr(VI) ions damages PVDF-based PIMs [27] (**Fig. 6a**) and, thus, limits their reuse.

The stability of PVDF-based PIM is also evaluated by the method proposed by O'Bryan [28], which consists in the membrane weighing after each cycle in order to determine the leakage rate of the liquid components. In our case, only negligible changes of the membrane weight and its thickness were observed. Indeed, the membrane lost only 8.7% of its initial weight after 24 cycles of the Cr(VI) transport and its thickness changed from 30.3 ± 2.3 µm for the fresh membrane to 28.7 ± 2.3 µm after 24 cycles (i.e. for 192h).

In order to quantify the possible leakage of the liquid components (i.e. ion carrier and/or plasticizer) from PVDF-based PIM, the 75PVDF/20Aliquat 336/5-2NPOE membrane was immersed in different media used as the donor and acceptor phases in the case of the Cr(VI) transport measurements (namely, milli-Q water, 0.1 M HCl and buffer solution of acetic acid/ammonium acetate at pH 5) and its weight was monitored (**Fig. 10b**). During the membrane immersion in water its weight decreased rapidly during first hours because of the ion carrier and/or plasticizer leakage, but starting from 50h, the membrane weight was stabilized. 75PVDF/20Aliquat 336/5-2NPOE membrane lost ~10% of its initial weight that represents ~40% of the mass of its liquid components. It should be noted that the stability of PVDF-based PIM in water is much better than the stability of PVC-based PIM studied by Kagaya et al. as in that case the loss of 30% of the membrane initial weight was observed, i.e. more than 80% of the weight of Aliquat 336 [55]. This result can be explained by the better miscibility of Aliquat 336 with PVDF than with PVC [56]. The noted intermolecular interactions of components of PVDF-based PIM (**Fig. 1a**) and strong electrostatic interactions

between the liquid compounds and the PVDF polymer chains (**Table 2**) are the proofs of good miscibility and compatibility of PVDF with Aliquat 336.

When the membrane is immersed in 0.1 M HCl, its weight loss is reduced and presents less than 3%. Moreover, when the membrane is immersed in buffer solution of acetic acid/ammonium acetate (pH 5) its weight remains constant (**Fig. 10b**). As the loss of the liquid phase from PIMs depends on the medium nature and its ion concentration [55, 57], this leakage will be the smallest for the solution with the highest ionic strength [57]. The high stability of PVDF-based PIM during immersion in acetic acid/ammonium acetate buffer solution (i.e. in acceptor phase) is in the origin of its stability during repeated Cr(VI) transport (**Fig. 10a**).

In order to increase the membrane stability several methods can be proposed [55-58]. Among them, one can noted the elaboration of gel-like PIMs, membranes containing different inorganic charges thus preventing the carrier leakage, and/or grafting of the carrier the polymer backbone. In each case different advantages and limitations can be observed, so, the compromise between mechanical properties and transport performance should be found.

The stability of 75PVDF/20Aliquat 336/5-2NPOE membrane was also determined by the mechanical properties. For this purpose, the stress-strain curves for the fresh membrane, after one cycle and 24 cycles of the Cr(VI) permeability measurements were obtained (not shown). After one cycle of the Cr(VI) transport, the membrane mechanical properties stayed practically unchanged (i.e. elongation at break = 302%, strength at break = 15.6 MPa, Young's modulus = 438.9 MPa) compared to the fresh membrane (**Table 1**). This result confirms that the membrane remains in its initial state, i.e. the liquid components loss is negligible. However, after 24 cycles, the membrane tensile strength increases up to 20.2MPa, its Young's modulus also increases to 750.9 MPa, and its elongation at break is reduced to ~25%. Such increase of the membrane mechanical behavior is certainly due to the loss of a certain quantity of membrane liquid components (**Fig. 10a**).

3.2.6. Membrane durability and lifetime studies

To study the stability and durability of PVDF-based PIMs over time, the membranes were stored several months at room temperature (24 ± 2°C) and relative humidity (34 ± 5%) and the transport experiments were carried out periodically. The evolution of the Cr(VI) concentration in the donor and acceptor phases for PVDF-based PIMs is plotted in **Fig. 11**. It can be seen that PIMs preserve their transport efficiency after 9 and 18 months of storage whatever the membrane composition. This result testifies to the membrane durability. The performed TGA analysis reveals that the aged membranes keep their liquid compounds – about 25% for 75PVDF/20Aliquat 336/5-2NPOE membrane and about 30% for 70PVDF/30Aliquat 336 membrane. The membrane elastic behaviour was not really changed after 18 months of storage as the following values were obtained: Young's modulus of 417.5 MPa, strength at break = 16.8 MPa, elongation at break = 259.5% for 75PVDF/20Aliquat 336/5-2NPOE and Young's modulus = 258 MPa, strength at break = 13.1MPa, elongation at break = 235.4% for 70PVDF/30Aliquat 336. These values are very close to the mechanical behaviour of the fresh membranes (**Table 1**). Visually, the surfaces of the aged membranes are similar to those of the fresh membranes and are not oily, which means that the liquid compounds were not leaked out

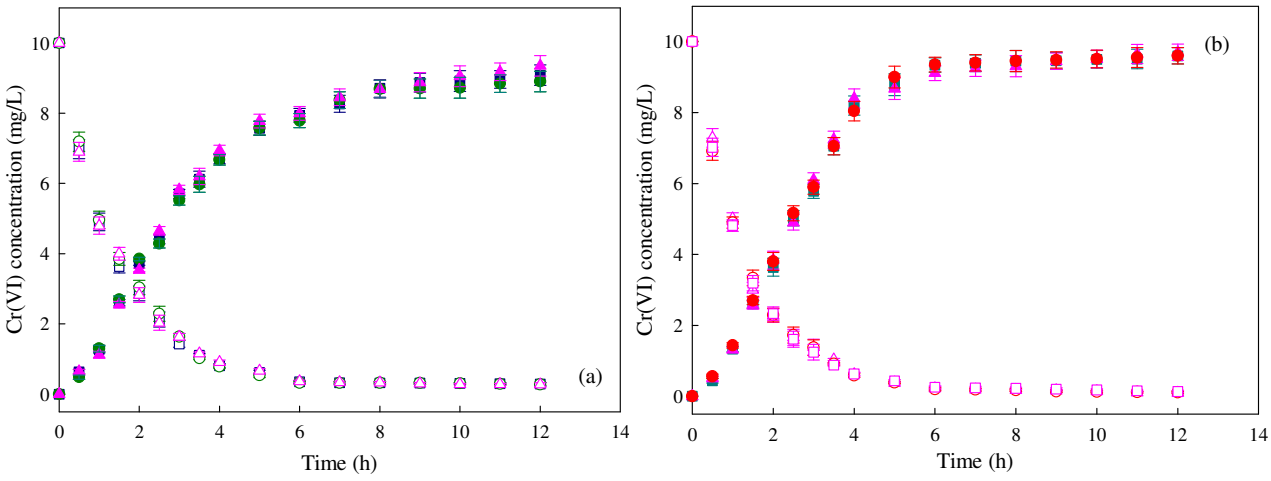

Fig. 11. Transient Cr(VI) concentration curves for the feed (open symbols) and stripping (filled symbols) phases for (□) fresh, (*o*) aged 9 months and (*Δ*) aged 18 months membranes: *(a)* 70PVDF/30Aliquat 336, (*b*) 75PVDF/20Aliquat 336/5-2NPOE.

from the membrane during storage. The water contact angle measurements carried out for the aged membranes didn't show any variation in water contact angle values compared to the fresh membranes indicating the good stability of PIMs over time. In fact, the PIM liquid compounds are trapped in a polymer matrix, thus inhibiting the leaching of the ion carrier.

Moreover, as demonstrated by FTIR and thermal analysis, the intermolecular and strong electrostatic interactions between the liquid components and the polymer chains (such as van der Waals or hydrogen bonds) contribute to maintain the liquid compounds inside the membrane, thus increasing its stability and durability.

Conclusion

PVDF-based PIMs containing Aliquat 336 as an ion carrier and 2NPOE as a plasticizer designed for the Cr(VI) transport were successfully elaborated by the solvent evaporation technique and the membrane composition was optimized in terms of mechanical and transport properties. As revealed by microscopy, thermal and FTIR analysis, the dense and homogeneous membranes with strong electrostatic interactions between the different components (i.e. base polymer, ion carrier and plasticizer) were obtained. It was found that the ion carrier quantity had a strong influence on the membrane mechanical properties, hydrophobic/hydrophilic character and, consequently, on the Cr(VI) transport performance. Moreover, the addition of small amount of the plasticizer (2NPOE) (only 5 wt.%) improved significantly the initial flux of the Cr(VI) ions transport– from 3.8 µmol/(m²·s) for 80PVDF/20Aliquat 336 to 5.6 µmol/(m²·s) for 75PVDF/20Aliquat 336/5-2NPOE. It was found that the membrane based on 75% PVDF, 20%Aliquat 336 and 5% 2NPOE selectively transported Cr(VI) ions (96.9%). Besides, the increase of the initial Cr(VI) concentration in the feed phase had also a positive influence on the transport flux. The performance of PVDF-based PIM was compared to PIMs based on conventional polymers, such as CTA and PVC, and much better transport properties, life time stability and durability were revealed. Also, the results of the aging study testified to the fact that PVDF-based PIM preserved its elastic behavior and transport capacity towards Cr(VI) ions up to 18 months. Thus, the results presented in this work indicate the excellent selectivity and stability of PVDF-based PIM, making it a promising candidate in areas of ion separation and water treatment.

Acknowledgement

F. Sellami acknowledges the University of Bejaia (Algeria) and Algerian Government for the financial support of his PhD thesis (Short-term Scientific internship and PNE 2016-2017).

References

1. F.C. Richard, A.C.M. Bourg, Aqueous geochemistry of chromium: a review // Water Res., 25 (1991), pp. 807-816.
2. D.C. Sharma, C.F. Forster, Column studies into the adsorption of chromium (VI) using sphagnum moss peat // Bioresour. Technol., 52 (1995), pp. 261-267.
3. G.M. Gadd, C. White, Microbial treatment of metal pollution — a working biotechnology? // Trends Biotechnol., 11 (1993), pp. 353-359.
4. P. Miretzky, A.F. Cirelli, Cr(VI) and Cr(III) removal from aqueous solution by raw and modified lignocellulosic materials: a review // J. Hazard. Mater., 180 (2010), pp. 1-19.
5. H. Sereshti, M.V. Farahani, M. Baghdadi, Trace determination of chromium (VI) in environmental water samples using innovative thermally reduced graphene (TRG) modified SiO_2 adsorbent for solid phase extraction and UV–vis spectrophotometry // Talanta, 146 (2016), pp. 662-669.
6. United States Environmental Agency, Drinking water contaminants – standards and regulations. Available online: http://www.epa.gov/safewater/contaminants/index.html; (accessed on 9 May 2019).
7. M.I.G.S. Almeida, R.W. Cattrall, S.D. Kolev, Recent trends in extraction and transport of metal ions using polymer inclusion membranes (PIMs) // J. Membr. Sci., 415-416 (2012), pp. 9-23.
8. S. Rengaraj, K.H. Yeon, S.H. Moon, Removal of chromium from water and wastewater by ion exchange resins // J. Hazard. Mater., 87 (2001), pp. 273-287.
9. L. Wu, L. Liao, G. Lv, F. Qin, Y. He, X. Wang, Micro-electrolysis of Cr(VI) in the nanoscale zero-valent iron loaded activated carbon // J. Hazard. Mater., 254 (2013), pp. 277-283.
10. Z. Guo, J. Zhang, H. Liu, Y. Kang, Development of a nitrogen-functionalized carbon adsorbent derived from biomass waste by diammonium hydrogen phosphate activation for Cr(VI) removal // Powder Technol., 318 (2017), pp. 459-464.
11. L. Fischer, T. Falta, G. Koellensperger, A. Stojanovic, D. Kogelnig, M. Galanski, R. Krachler, B.K. Keppler, S. Hann, Ionic liquids for extraction of metals and metal containing compounds from communal and industrial waste water // Water Res., 45 (2011), pp. 4601-4614.
12. M. O'Rourke, R.W. Cattrall, S.D. Kolev, I.D. Potter, The extraction and transport of organic molecules using polymer inclusion membrane // Solvent Extr. Res. Dev., Jpn., 16 (2009), pp. 1-12.

13. F. Sellami, O. Kebiche-Senhadji, S. Marais, N. Couvrat, K. Fatyeyeva, Polymer inclusion membranes based on CTA/PBAT blend containing Aliquat 336 as extractant for removal of Cr(VI): efficiency, stability and selectivity // React. Function. Polym., 139 (2019), pp. 120-132.

14. C.-V.I. Gherasim, G. Bourceanu, R.-I. Olariu, C. Arsene, Removal of lead(II) from aqueous solutions by a polyvinyl-chloride inclusion membrane without added plasticizer // J. Membr. Sci., 377 (2011), pp. 167-174.

15. L.D. Nghiem, P. Mornane, I.D. Potter, J.M. Perera, R.W. Cattrall, S.D. Kolev, Extraction and transport of metal ions and small organic compounds using polymer inclusion membranes (PIMs) // J. Membr. Sci., 281 (2006), pp. 7-41.

16. Y.Y.N. Bonggotgetsakul, R.W. Cattrall, S.D. Kolev, Recovery of gold from aqua regia digested electronic scrap using a poly(vinylidene fluoride-*co*-hexafluoropropene) (PVDF-HFP) based polymer inclusion membrane (PIM) containing Cyphos® IL 104 // J. Membr. Sci., 514 (2016), pp. 274-281.

17. N. Pereira, A. St John, R.W. Cattrall, J.M. Perera, S.D. Kolev, Influence of the composition of polymer inclusion membranes on their homogeneity and flexibility // Desalination, 236 (2009), pp. 327-333.

18. J.S. Gardner, J.O. Walker, J.D. Lamb, Permeability and durability effects of cellulose polymer variation in polymer inclusion membranes // J. Membr. Sci., 229 (2004), pp. 87-93.

19. P.K. Mohapatra, D.S. Lakshmi, A. Bhattacharyya, V.K. Manchanda, Evaluation of polymer inclusion membranes containing crown ethers for selective cesium separation from nuclear waste solution // J. Hazard. Mater., 169 (2009), pp. 472-479.

20. H. Kise, Dehydrochlorination of poly(vinyl chloride) by aqueous sodium hydroxide solution under two-phase conditions // J. Polym. Sci. Polym. Chem. Ed., 20 (1982), pp. 3189-3197.

21. O. Kebiche-Senhadji, S. Tingry, P. Seta, M. Benamor, Selective extraction of Cr(VI) over metallic species by polymer inclusion membrane (PIM) using anion (Aliquat 336) as carrier // Desalination, 258 (2010), pp. 59-65.

22. D. Wang, J. Hu, Y. Li, M. Fu, D. Liu, Q. Chen, Evidence on the 2-nitrophenyl octyl ether (NPOE) facilitating copper(II) transport through polymer inclusion membranes // J. Membr. Sci., 501 (2016), pp. 228-235.

23. F. Liu, N.A. Hashim, Y. Liu, M.R.M. Abed, K. Li, Progress in the production and modification of PVDF membranes // J. Membr. Sci., 375 (2011), pp. 1-27.

884 24. G. Kang, Y. Cao, Application and modification of poly(vinylidene fluoride) (PVDF)
885 membranes – a review // J. Membr. Sci., 463 (2014), pp. 145-165.
886 25. L. Guo, J. Zhang, D. Zhang, Y. Liu, Y. Deng, J. Chen, Preparation of poly(vinylidene
887 fluoride-*co*-tetrafluoroethylene)-based polymer inclusion membrane using bifunctional ionic
888 liquid extractant for Cr(VI) transport // Ind. Eng. Chem. Res., 51 (2012), pp. 2714-2722.
889 26. L. Guo, Y. Liu, C. Zhang, J. Chen, Preparation of PVDF-based polymer inclusion
890 membrane using ionic liquid plasticizer and Cyphos IL 104 carrier for Cr(VI) transport // J.
891 Membr. Sci., 372 (2011), pp. 314-321.
892 27. L. Chen, J. Chen, Asymmetric membrane containing ionic liquid [A336][P507] for the
893 preconcentration and separation of heavy rare earth lutetium // ACS Sustain. Chem. Eng., 4
894 (2016), pp. 2644-2650.
895 28. Y. O'Bryan, R.W. Cattrall, Y.B. Truong, I.L. Kyratzis, S.D. Kolev, The use of
896 poly(vinylidenefluoride-*co*-hexafluoropropylene) for the preparation of polymer inclusion
897 membranes. Application to the extraction of thiocyanate // J. Membr. Sci., 510 (2016), pp.
898 481-488.
899 29. M.R. Yaftian, M.I.G.S. Almeida, R.W. Cattrall, S.D. Kolev, Selective extraction of
900 vanadium(V) from sulfate solutions into a polymer inclusion membrane composed of
901 poly(vinylidenefluoride-*co*-hexafluoropropylene) and Cyphos® IL 101 // J. Membr. Sci., 545
902 (2018), pp. 57-65.
903 30. H.I. Turgut, V. Eyupoglu, R.A. Kumbasar, I. Sisman, Alkyl chain length dependent
904 Cr(VI) transport by polymer inclusion membrane using room temperature ionic liquids as
905 carrier and PVDF-*co*-HFP as polymer matrix // Sep. Purif. Technol., 175 (2017), pp. 406-417.
906 31. D. Wang, R.W. Cattrall, J. Li, M.I.G.S. Almeida, G.W. Stevens, S.D. Kolev, A
907 comparison of the use of commercial and diluent free LIX84I in poly(vinylidene fluoride-*co*-
908 hexafluoropropylene) (PVDF-HFP)-based polymer inclusion membranes for the extraction
909 and transport of Cu(II) // Sep. Purif. Technol., 202 (2018), pp. 59-66.
910 32. M.L. Yeow, Y.T. Liu, K. Li, Morphological study of poly(vinylidene fluoride)
911 asymmetric membranes: effects of the solvent, additive, and dope temperature // J. Appl.
912 Polym. Sci., 92 (2004), pp. 1782-1789.
913 33. T. Boccaccio, A. Bottino, G. Capannelli, P. Piaggio, Characterization of PVDF
914 membranes by vibrational spectroscopy // J. Membr. Sci., 201 (2002), pp. 315-329.
915 34. J.C.C. Ferreira, T.S. Monteiro, A.C. Lopes, C.M. Costa, M.M. Silva, A.V. Machado,
916 S. Lanceros-Mendez, Variation of the physicochemical and morphological characteristics of

917 solvent casted poly(vinylidene fluoride) along its binary phase diagram with
918 dimethylformamide // J. Non-Cryst. Solids, 412 (2015), pp. 16-23.
919 35. G. Naz, Z. Othaman, M. Shamsuddin, S.K. Ghoshal, Aliquat 336 stabilized multi-faceted
920 gold nanoparticles with minimal ligand density // Appl. Surf. Sci., 363 (2016), pp. 74-82.
921 36. H. Cui, J. Chen, H. Yang, W. Wang, Y. Liu, D. Zou, W. Liu, G. Men, Preparation and
922 application of Aliquat 336 functionalized chitosan adsorbent for the removal of Pb(II) //
923 Chem. Eng. J., 232 (2013), pp. 372-379.
924 37. O. Kebiche-Senhadji, L. Mansouri, S. Tingry, P. Seta, M. Benamor, Facilitated Cd(II)
925 transport across CTA polymer inclusion membrane using anion (Aliquat 336) and cation
926 (D2EHPA) metal carriers // J. Membr. Sci., 310 (2008), pp. 438-445.
927 38. V.K. Thakur, M.-F. Lin, E.J. Tan, P.S. Lee, Green aqueous modification of
928 fluoropolymers for energy storage applications // J. Mater. Chem., 22 (2012), pp. 5951-5959.
929 39. F. He, B. Luo, S. Yuan, B. Liang, C. Choong, S. Olavi Pehkonen, PVDF film tethered
930 with RGD- click -poly(glycidyl methacrylate) brushes by combination of direct surface-
931 initiated ATRP and click chemistry for improved cytocompatibility // RSC Adv., 4 (2014),
932 pp. 105-117.
933 40. R. Gregorio, D.S. Borges, Effect of crystallization rate on the formation of the
934 polymorphs of solution cast poly(vinylidene fluoride) // Polymer, 49 (2008), pp. 4009-4016.
935 41. Y.K.A. Low, N. Meenubharathi, N.D. Niphadkar, F.Y.C. Boey, K.W. Ng, α- and β-
936 poly(vinylidene fluoride) evoke different cellular behaviours // J. Biomater. Sci. Polym. Ed.,
937 22 (2011), pp. 1651-1667.
938 42. R. Mejri, J.C. Dias, A.C. Lopes, S. Bebes Hentati, M.M. Silva, G. Botelho, A. Mão de
939 Ferro, J.M.S.S. Esperança, A. Maceiras, J.M. Laza, J.L. Vilas, L.M. León, S. Lanceros-
940 Mendez, Effect of ionic liquid anion and cation on the physico-chemical properties of
941 poly(vinylidene fluoride)/ionic liquid blends // Eur. Polym. J., 71 (2015), pp. 304-313.
942 43. Z. Dong, Q. Zhang, C. Yu, J. Peng, J. Ma, X. Ju, M. Zhai, Effect of ionic liquid on the
943 properties of poly(vinylidene fluoride)-based gel polymer electrolytes // Ionics, 19 (2013), pp.
944 1587-1593.
945 44. H.Z. Chen, P. Li, T.-S. Chung, PVDF/ionic liquid polymer blends with superior
946 separation performance for removing CO_2 from hydrogen and flue gas // Int. J. Hydrog.
947 Energy, 37 (2012), pp. 11796-11804.
948 45. M.E. Achaby, F.-E. Arrakhiz, S. Vaudreuil, E.M. Essassi, A. Qaiss, M. Bousmina,
949 Nanocomposite films of poly(vinylidene fluoride) filled with polyvinylpyrrolidone-coated

multiwalled carbon nanotubes: enhancement of β-polymorph formation and tensile properties // Polym. Eng. Sci., 53 (2013), pp. 34-43.

46. M.I. Vázquez, V. Romero, C. Fontàs, E. Anticó, J. Benavente, Polymer inclusion membranes (PIMs) with the ionic liquid (IL) Aliquat 336 as extractant: effect of base polymer and IL concentration on their physical–chemical and elastic characteristics // J. Membr. Sci., 455 (2014), pp. 312-319.

47. I. Iben Nasser, F. Ibn El Haj Amor, L. Donato, C. Algieri, A. Garofalo, E. Drioli, C. Ahmed, Removal and recovery of $Ag(CN)_2^-$ from synthetic electroplating baths by polymer inclusion membrane containing Aliquat 336 as a carrier // Chem. Eng. J., 295 (2016), pp. 207-217.

48. A. Kuila, N. Maity, D.P. Chatterjee, A.K. Nandi, Temperature triggered antifouling properties of poly(vinylidene fluoride) graft copolymers with tunable hydrophilicity // J. Mater. Chem. A, 3 (2015), pp. 13546-13555.

49. C.A. Kozlowski, W. Walkowiak, Applicability of liquid membranes in chromium(VI) transport with amines as ion carriers // J. Membr. Sci., 266 (2005), pp. 143-150.

50. C. Deferm, A.V. den Bossche, J. Luyten, H. Oosterhof, J. Fransaer, K. Binnemans, Thermal stability of trihexyl(tetradecyl)phosphonium chloride // Phys. Chem. Chem. Phys., 20 (2018), pp. 2444-2456.

51. A. Kaya, C. Onac, H.K. Alpoğuz, S. Agarwal, V.K. Gupta, N. Atar, A. Yilmaz, Reduced graphene oxide based a novel polymer inclusion membrane: transport studies of Cr(VI) // J. Mol. Liq., 219 (2016), pp. 1124-1130.

52. C.-V. Gherasim, G. Bourceanu, R.-I. Olariu, C. Arsene, A novel polymer inclusion membrane applied in chromium (VI) separation from aqueous solutions // J. Hazard. Mater., 197 (2011), pp. 244-253.

53. A. Kaya, C. Onac, H.K. Alpoguz, A. Yilmaz, N. Atar, Removal of Cr(VI) through calixarene based polymer inclusion membrane from chrome plating bath water // Chem. Eng. J., 283 (2016), pp. 141-149.

54. Y. O'Bryan, Y.B. Truong, R.W. Cattrall, I.L. Kyratzis, S.D. Kolev, A new generation of highly stable and permeable polymer inclusion membranes (PIMs) with their carrier immobilized in a crosslinked semi-interpenetrating polymer network. Application to the transport of thiocyanate // J. Membr. Sci., 529 (2017), pp. 55-62.

55. S. Kagaya, Y. Ryokan, R.W. Cattrall, S.D. Kolev, Stability studies of poly(vinyl chloride)-based polymer inclusion membranes containing Aliquat 336 as a carrier // Sep. Purif. Technol., 101 (2012), pp. 69-75.

984 56. N.-S. Abdul-Halim, P.G. Whitten, L.D. Nghiem, Characterizing poly(vinyl
985 chloride)/Aliquat 336 polymer inclusion membranes: evidence of phase separation and its role
986 in metal extraction // Sep. Purif. Technol., 119 (2013), pp. 14-18.
987 57. L.L. Zhang, R.W. Cattrall, M. Ashokkumar, S.D. Kolev, On-line extractive separation
988 in flow injection analysis based on polymer inclusion membranes: a study on membrane
989 stability and approaches for improving membrane permeability // Talanta, 97 (2012), pp. 382-
990 387.
991 58. J. Song, T. Huang, H. Qiu, X. Niu, X.-M. Li, Y. Xie, T. He, A critical review on
992 membrane extraction with improved stability: potential application for recycling metals from
993 city mine // Desalination, 440 (2018), pp. 18-38.
994
995